Published in final edited form as:
J Magn Reson Imaging. 2014 January ; 39(1): . doi:10.1002/jmri.24130.

Impact of Reduced k-Space Acquisition on Pathologic Detectability for Volumetric MR Spectroscopic Imaging

Mohammad Sabati, PhD[1], **Jiping Zhan, PhD**[1], **Varan Govind, PhD**[1], **Kristopher L. Arheart, PhD**[2], and **Andrew A. Maudsley, PhD**[1]

[1]Department of Radiology, Miller School of Medicine, University of Miami, Miami, FL 33136

[2]Department of Epidemiology and Public Health, Miller School of Medicine, University of Miami, Miami, FL 33136

Abstract

Purpose—To assess the impact of accelerated acquisitions on the spectral quality of volumetric MR spectroscopic imaging (MRSI) and to evaluate their ability in detecting metabolic changes with mild injury.

Materials and Methods—The implementation of a generalized autocalibrating partially parallel acquisition (GRAPPA) method for a high-resolution whole-brain echo planar SI (EPSI) sequence is first described and the spectral accuracy of the GRAPPA-EPSI method is investigated using lobar and voxel-based analyses for normal subjects and patients with mild traumatic brain injuries (mTBI). The performance of GRAPPA was compared with that of fully-encoded EPSI for 5 datasets collected from normal subjects at the same scanning session, as well as on 45 scans (20 normal subjects and 25 mTBI patients) for which the reduced k-space sampling was simulated. For comparison, a central k-space lower-resolution 3D-EPSI acquisition was also simulated. Differences in individual metabolites and metabolite ratio distributions of the mTBI group relative to those of age-matched control subjects were statistically evaluated using analyses divided into hemispheric brain lobes and tissue types.

Results—GRAPPA-EPSI with 16-min scan time yielded robust and similar results in terms of MRSI quantitation, spectral fitting, and accuracy with that of fully sampled 3D-EPSI acquisitions and was more accurate than central k-space acquisition. Primary findings included high correlations (accuracy of 92.6%) between the GRAPPA and fully sampled results.

Conclusion—Although the reduced encoding method is associated with lower SNR that impact the quality of spectral analysis the use of parallel imaging method can lead to same diagnostic outcomes as of the fully sampled data when using the sensitivity-limited volumetric MRSI.

Keywords

MR spectroscopic imaging; parallel Imaging; traumatic brain injury; undersampled acquisition; clinical equivalency

INTRODUCTION

Magnetic resonance spectroscopic imaging (MRSI) enables noninvasive assessment of the spatial distribution of different metabolites and is widely used for evaluation of neurological diseases and injury (1–3). Although widely implemented as a 2D acquisition, the echo-

Correspondence to: Mohammad Sabati, PhD, Department of Radiology, Miller School of Medicine, University of Miami, 1150 NW 14 Street, Suite 713, Miami, FL 33136, Tel: 305-243-7458, Fax: 305-243-3405, msabati@med.miami.edu.

planar spectroscopic imaging (EPSI) method is an efficient data acquisition approach that can be used to obtain 3D maps of brain metabolite distributions (4). It provides improved sampling efficiency by simultaneously encoding the spectral dimension together with one spatial dimension, thus reducing the time-consuming spatial encoding to two dimensions. However, when high spatial resolution is desired the 3D EPSI can still be limited by relatively long scan times that are undesirable for many clinical settings.

Parallel MR imaging (PI) techniques (5–7) enable a reduction in imaging time by utilizing the spatial information inherent in the non-uniform spatial sensitivities of a multichannel phased-array coil to account for missing phase-encoding information. Parallel MRI techniques have been used with both standard phase-encoded MRSI (8–10) and fast MRSI (11–16) to reduce data acquisition times. Of the available PI reconstruction strategies the generalized autocalibrating partially parallel acquisitions (GRAPPA) method (7) has been shown to provide greater flexibility for accurate and coherent spectral phase alignment (12, 13) avoiding potential artifacts and phase cancellations of the metabolite signals. To avoid the problem of spectral line-broadening and distortion encountered in magnitude-based, sum-of-squares, GRAPPA MRSI methods (17) and to diminish possible phase cancellation of the metabolite signals, Zhu *et al.* (12) proposed to use a complex image reconstruction method (18) following a frequency domain phase correction approach, termed “spectral phase correction in GRAPPA” (SPC-GRAPPA). Considerable improvement compared to the conventional GRAPPA-EPSI implementation was achieved. Although the quality of the spectral fitting and signal-to-noise (SNR) performance of the SPC-GRAPPA was validated on a limited number of simulated datasets, the comparison with the fully sampled data was carried out for only a small region of the brain, which did not take into account spatial variations of metabolite concentrations and detection sensitivity. Another limitation in all simulated reduced k-space acquisitions is that they often result in unrealistic SNR comparative values.

The use of a reduced phase encoding strategy inevitably comes at the expense of reduced SNR, due to shorter scan time and phased-array coil geometry-factor in PI (6), and may alter the appearance of potential image artifacts. Although PI methods are widely used for diagnostic MRI applications these are for the most part not as sensitivity-limited as MRSI methods, and few reports have studied the resultant impact that PI may have when applied to MRSI on the outcome of clinical studies or diagnostic accuracy compare to the fully sampled MRSI data.

A study by Zierhut *et al.* (19) compared 3D MRSI using ellipsoidal *k*-space encoding, SENSE MRSI, and EPSI, which confirmed the SNR reduction with the PI acquisition and concluded that all techniques could potentially produce spectroscopic images that are qualitatively acceptable for clinical applications. Ozturk-Isik *et al.* (10) also showed the effectiveness of SENSE parallel imaging MRSI in patients with high-grade glioma tumors. However, for these studies the relative performance for the reduced k-space acquisition variants remained well within that required for the target pathologies, where large alterations of the brain metabolites can occur, and the moderate spatial resolutions used for which good SNR values could still be obtained. Therefore, the use of reduced k-space techniques requires further evaluation for applications where larger numbers of k-space points are required, as well as for target pathologies for which metabolite alterations are relatively small.

It therefore remains unknown whether the clinical diagnostic value is maintained for PI implementations MRSI, i.e. is the ability to detect subtle pathology equivalent to that of the fully-sampled MRSI method? In this study, this question is addressed by first implementing an improvement to the GRAPPA-EPSI method within a fully-automated volumetric MRSI

data processing pipeline, and then evaluating this method using studies of healthy volunteers and subjects with mild traumatic brain injury (mTBI), which represents a patient group for which the metabolic changes are relatively diffuse and frequently can only be determined using quantitative assessments (20, 21). The performance of the GRAPPA implementation in terms of quantitation accuracy is compared with that of fully sampled volumetric EPSI data collected at the same session from five healthy subjects. Next, the effect of GRAPPA on lobar and voxel-based regional analyses for mTBI compared to age-matched control group was evaluated, with individual metabolite images reconstructed from the fully sampled 3D EPSI acquisitions used as the gold standard. An additional comparison was carried out for a reduced spatial resolution 3D ESPI with a scan time matched to that of the GRAPPA acquisition. The null-hypothesis tested in this study is that, from the clinical decision viewpoints, the reduced k-space volumetric MRSI produces results that are equivalent to that of the fully acquired MRSI data.

MATERIALS AND METHODS

Subject Selection

Twenty-five subjects (22M/3F, age: 25.76±4.23, age range: 20–34) that had experienced a mild TBI (Glasgow Coma Score of 13 to 15) were retrospectively selected from an existing group of subjects. Details of the subject enrollment criteria are described in a previous report (21). The MR scan was performed at least one week post-injury ranging 7 to 75 days and the median time of the study after injury was 28 days. Additional studies were carried out for five normal subjects (3M/2F, age: 28.60±3.91, age range: 25–35) that underwent both fully-sampled and GRAPPA-EPSI scans (Group 1). These normal subject data were also combined with twenty datasets (13M/7F, age: 27.70±3.25, age range: 22–33) from an existing database (22) (Group 2), for a total of 25 age-matched control subjects. The study protocol was approved by the institutional review board and all subjects provided signed written consent before participation.

Data Acquisition

MR data were acquired at 3.0 Tesla (Siemens Tim/Trio, Erlangen, Germany) using an eight-channel phased-array receiver coil (InVivo Corporation, Gainesville, FL, USA). For full k-space sampling MRSI data were collected using a volumetric spin-echo EPSI sequence with chemical shift-selective water suppression, lipid inversion nulling with TI = 198 ms, excitation angle of 73° for a 135-mm slab, TE/TR = 70 ms/1710 ms, FOV= 280×280×180 mm^3, k-space points = 50 [read] × 50 [phase] ×18 [slice], nominal voxel size of 5.6×5.6×10 mm^3 = 0.31 mL, spectral sweep width 1250 Hz, and total acquisition time of 26 min. With each coil element a metabolite EPSI dataset was acquired that consisted of 1000 sampling points of the FID signal. The acquisition included an interleaved water reference acquisition of the same dimensions as the metabolite data obtained using a gradient-echo acquisition with 20° excitation angle and TE = 6.3 ms (22). The MR protocol also included a T1-weighted MRI (MPRAGE; TE/TR= 4.43 ms/2150 ms, 160 slices, 1-mm slice thickness, FOV: 256×256mm^2, and acquisition time of 5 min). The MRI and MRSI acquisitions were performed at the same angulations, with the slice or slab orientations of all acquisitions angulated at +15-deg from the anterior commissure – posterior commissure plane. For the reduced k-space acquisition the 3D EPSI sequence was modified to acquire only 32 phase-encoding lines in the k_y direction with a subsampling factor of 2 and seven additional autocalibration lines centered around $k_y = 0$ achieving an acceleration factor of 1.5. The MRSI data acquisition time was therefore reduced to 16.4 min.

The performance of the GRAPPA-enabled 3D EPSI sequence was compared with that of fully sampled 3D EPSI data by collecting both of these EPSI datasets in the same session on

five healthy subjects (Group 1) for whom the GRAPPA-EPSI acquisition was also simulated. To evaluate the performance of the pathologic detectability of GRAPPA-MRSI reconstructions and to assess its variability and quantitative accuracy, a reduced k-space acquisition was simulated on the fully sampled 3D EPSI data, for both the metabolite and water-reference acquisitions, obtained from all the mTBI patients and twenty aged-matched normal subjects (Group 2). This was achieved by removing the same phase-encoding measurements as implemented for the reduced k-space pulse sequence and bringing k_y to 32 as described above. A low-resolution central k-space MRSI data with contiguous 32 phase encoding lines (to match the scan time of the GRAPPA acquisition) was also simulated and evaluated for comparisons.

Data Reconstruction and Processing

MRSI data were processed in a fully-automated manner using the MIDAS package (23). Fully-sampled EPSI data processing and reconstruction was carried out using standard Fourier transform reconstruction and phase-sensitive multichannel combination using the phase and magnitude information derived from the water reference SI. To handle the undersampled data a modified GRAPPA reconstruction algorithm based on the method of Zhu *et al.* (12) was implemented as part of the MIDAS MRSI data processing package (23). The SPC-GRAPPA was modified to apply the GRAPPA reconstruction algorithm developed by Griswold *et al.* (7) to the undersampled metabolite and water reference k-space data at each time-point of the FID prior to any spatial Fourier transformation. Secondly, rather than obtaining the GRAPPA reconstructing kernel weights from a single time-point of the FID signals and then using the same weights for the GRAPPA reconstruction of other time-points, the weights were determined at each time-point of FID for a GRAPPA reconstruction of that same time-point as this was shown to reduce noise amplification (18, 24). Following GRAPPA reconstruction of the unsampled k-space points the unfolded 3D complex water reference and metabolite images were reconstructed for each coil element. The metabolite data from each coil element were then combined after phase alignment in time domain using the phase and magnitude of the water reference images (25).

Metabolite image reconstruction also included spatial smoothing and interpolation to 64×64×32 voxels, with a resultant voxel volume of approximately 1 mL and automatic spectral fitting. The processing steps included calculation of the MRSI voxel tissue content based on tissue segmentation of the high-resolution T1-weighted MRI; voxel-by-voxel metabolite signal normalization to the internal water reference data (represented in and commonly known as institutional unit); and spatial registration to the simulated Montréal Neurological Institute MRI template (26), which was matched to a brain atlas that delineated eight hemispheric lobes (right and left frontal, temporal, parietal, and occipital) and the cerebellum (23).

Data Analyses and Statistical Tests

To evaluate the quantitative results and the accuracy of the reduced k-space data the fully sampled 3D EPSI data were reconstructed as a gold standard. Spectral fitting was used to obtain the relative concentration of N-acetyl aspartate (NAA), creatine (Cre), and choline (Cho), together with an estimation of the goodness-of-the-fit quantified by the individual metabolite Cramer-Rao lower bounds (CRLB) (27) at each voxel, and amplitudes normalized using tissue water as a reference. The performance of GRAPPA and central k-space reconstructions was also estimated by comparing the number of spectra in the whole brain that satisfied a spectral fitting criterion of spectral line-width between 2 Hz and 12 Hz.

Average values of the individual metabolites and their ratios (NAA/Cre, Cho/Cre, and Cho/NAA) were calculated for gray matter and white matter within each lobar brain region of the

cerebrum. Values of individual metabolites were first corrected for partial volume signal loss due to cerebral spinal fluid contribution at each voxel, and metabolite values corresponding to 100% of each tissue type were obtained using a regression of the metabolite value against the tissue content, for all voxels selected from that region (22). The following limiting criteria were applied to ensure that the data chosen were based on the quality of spectra: First, a line-width criterion was applied to only include voxels with fitted spectral line-width between 2 and 12 Hz. Next, a fractional tissue volume criterion was applied to only include voxels with underlying tissue volume of > 80%. Finally, an outlier exclusion criterion was applied to exclude voxels with metabolite values greater than three times the standard deviation of the corresponding metabolite value over all the voxels within the particular region. This last criterion was applied separately for each metabolite value and ratio. The line-width criterion typically excluded approximately ~ 35% of brain voxels, and a further ~ 1% of brain voxels were excluded by using the outlier rejection criterion.

Results for GRAPPA and central *k*-space acquisitions were compared with the gold standard using mean concentrations of NAA, Cre, and Cho in each lobar brain region for all normal (Group 2) and mTBI subjects and voxel-by-voxel concentrations over the whole-brain of all normal subject (from Group 1). The voxel metabolic concentrations within the whole brain from each normal subject were also used to calculate correlation coefficients to estimate pixel-by-pixel differences of metabolic concentrations among GRAPPA, central k-space, and the gold standard.

An analysis of covariance with a linear mixed-effect model, fixed methodology effects and subject-specific random effects, was then used to compare GRAPPA and central k-space acquisition results with reconstruction from full k-space data. Finally, SNR maps of the NAA peak were calculated for the three different reconstructions methods on all subjects.

A secondary analysis was carried out to assess the correlation between the clinical findings of the reduced k-space and the fully sampled MRSI results on the mTBI group using the individual metabolites of NAA and Cho and their ratio (Cho/NAA) over the whole brain. A previous analysis using these metabolites demonstrated widespread alterations in a between-group comparison of mTBI subjects against normal controls (21). The metabolite measures were compared between groups and methods using a two-way analysis of variance (ANOVA) (factor 1: group: control *vs.* mTBI and factor 2: method: full *vs.* GRAPPA *vs.* central k-space sampling). The aim of this sub-categorization was to identify the presence of any interaction between the reconstruction method used and the group of subjects under investigation. For all the statistical tests, p-values < 0.05 were considered significant. Finally, the specificity, sensitivity, and accuracy of the GRAPPA and the central k-space sampling were calculated and compared against the gold standard.

RESULTS

Metabolite Maps and Spectral Quality

Representative images from ten contiguous axial slices for the T1-weighted MRI, individual metabolites, and metabolite ratios are shown in Figure 1 to demonstrate the quality and spatial extent of the metabolite maps obtained with the GRAPPA and the full k-space 3D EPSI sequences. Data were acquired from a 26-year-old normal male subject. The interleaved water reference images, metabolite maps (NAA, Cre, Cho) and Cho/NAA ratio images are shown in rows 2 through 5, respectively. The GRAPPA-EPSI sequence produced images that are in consistent with those of fully sampled data. The contours surrounding the NAA images represent the outer edge of the brain parenchyma, and were obtained from their corresponding T1-weighted images. The black areas within the contours of the metabolite images indicate voxels classified as having inadequate quality for spectral analysis based on

a water linewidth of >20 Hz. Figure 1 also shows that most slices include good sampling of cortical surface gray-matter regions, while limited data quality is obtained from temporal and inferior frontal regions due to high magnetic susceptibility variations within these regions. The bright spots primarily located at the edges of the brain typically indicate voxels with errors in the spectral fitting, commonly caused by residual water or lipid signals, and these results will be excluded by the outlier removal filter applied in the analysis procedure.

Figure 2 shows representative spectra from two slices of a 22-year-old male mTBI subject (initial GCS score of 13, scanned 53 days after injury). Spectra from GRAPPA and full k-space reconstructions are shown side by side for comparison demonstrating similar results. The figure shows one each from voxels in the right and left parieto-occipital region indicated on the T1-weighted MRIs. Comparison of spectra from this subject to a control subject (a 25-year-old female) of Figure 3 indicates altered NAA and Cho concentration in both the GRAPPA and full-sampled k-space data. Additional discussion on the spectral findings for TBI subjects has been presented (21).

Quantitative Accuracy

Representative spectra at four voxels in fronto-temporal and occipital lobes gray matter and parieto-occipital and parietal lobes white matter from a normal subject are shown in Figure 3 for four different reconstruction methods, *i.e.*, fully sampled, acquired-GRAPPA, simulated-GRAPPA, and central k-space. The reduced k-space methods have maintained the general appearance of the spectra compare to the fully sampled data, although spectra reconstructed with central k-space, shown in Figure 3e, exhibit baseline variations indicating increased lipid contamination, and all reduced k-space acquisitions have lower SNR, shown in Figure 4, as expected (10). The spectra from the simulated GRAPPA are very similar to those from full k-space data, whereas those from the acquired GRAPPA show slightly different baselines (sometimes superior) from the full k-space data as they were acquired on a separate scan. Representative color-rendered NAA images and maps of the SNR for NAA, at a central slice for four different reconstruction methods are shown in Figure 4. The NAA images reconstructed from all four methods appear similar, although with some reduction in quality for the central k-space method. The SNR maps show no distinctive spatial patterns, but with an indication of higher values for the full k-space data and evidence of increased ringing effects with the central k-space result.

The fitted-volume measures for each method (i.e., the percentage of fitted voxels that meet the line-width, the tissue volume threshold, and the outlier exclusion criteria) and for each scanned group are listed in Table 1. There was no significant difference in fitted volume between all three methods (p-value > 0.15) in the mTBI group, whereas in both normal groups the number of voxels that were acceptable after fitting was significantly lower with the central k-space method (p-values < 0.001). The mean values of the individual metabolite concentrations in institutional units obtained from the white matter tissue of the atlas-mapped parietal lobe are also listed in Table 1 together with the mean SNR values calculated from all voxels located at a middle slice of the volumetric NAA maps. Both acquired GRAPPA and central k-space reconstructions yielded metabolite values similar to those of the gold standard dataset (p-values > 0.20); however, there was a non-significant trend for increasing mean values of brain metabolites for simulated GRAPPA (Group 2 and mTBI). Voxels reconstructed from full *k*-space EPSI data showed non-significantly higher SNR than central k-space data (0.11 < p-value < 0.30). The mean SNR values measured from both full *k*-space and central k-space data were significantly higher than those obtained with the GRAPPA (p-value < 0.005). There were no significant difference between the SNR of the acquired and the simulated GRAPPA data (p-value > 0.45). Average SNR reduction ranged

from 3.5% to 8.9% for central k-space and from 21.1% to 29.8% for GRAPPA method, compare to the fully sampled data.

In Figure 5 are shown regression plots that compare results of the spectral fitting for the acquired GRAPPA data and full *k*-space data for all voxels within the brain that passed the quality selection criteria, for a normal subject. Figure 5a–c shows the metabolite (NAA, Cre, and Cho) concentrations from the GRAPPA data plotted against those obtained from full k-space data. Linear regressions show a strong correlation between GRAPPA and the gold standard, with correlation coefficients of $R^2_{NAA} = 0.989$, $R^2_{\mathrm{Cre}} = 0.985$, and $R^2_{\mathrm{Cho}} = 0.971$. The correlation coefficients calculated from the pairs of central k-space and the gold standard were $R^2_{\mathrm{NAA}} = 0.940$, $R^2_{\mathrm{Cre}} = 0.926$, and $R^2_{\mathrm{Cho}} = 0.899$. Figure 5d illustrates the NAA metabolite line-width after the GRAPPA reconstruction plotted against the NAA line-width of the fully sampled results with a high correlation of 0.972 indicating a maintained high spectral resolution. Figure 5e shows the CRLB for the GRAPPA reconstruction versus the fully sampled data for the Cho metabolite. The CRLB regression indicates relatively decreased performance for the GRAPPA results; however, with values still largely falling within acceptable ranges. Similar results were obtained for the CRLB of NAA and Cre.

Diagnostic Power Assessment

Figure 6 illustrates the paired linear regression analyses of the mean metabolite concentrations of the reduced k-space data against the fully sampled results over all brain regions for the mTBI group. Each point on the graph represents a mean metabolite value at one atlas-registered brain lobe for one subject. No significant differences were found between the slopes and the intercepts of each of the GRAPPA (*p*-values > 0.344) and the central k-space (*p*-values > 0.460) against the full k-space data as illustrated in Figures 6a and 6b, respectively. GRAPPA and the gold standard comparison yielded strong correlation coefficients of $R^2_{NAA} = 0.954$, $R^2_{\mathrm{Cre}} = 0.924$, and $R^2_{\mathrm{Cho}} = 0.970$ for the normal subjects and $R^2_{NAA} = 0.978$, $R^2_{\mathrm{Cre}} = 0.958$, and $R^2_{\mathrm{Cho}} = 0.988$ for the mTBI group demonstrating a small variability induced by the GRAPPA method. The correlation coefficients calculated from the pairs of the central k-space data and the gold standard were $R^2_{NAA} = 0.960$, $R^2_{\mathrm{Cre}} = 0.976$, and $R^2_{\mathrm{Cho}} = 0.888$ with a noticeable larger variability than GRAPPA.

Average NAA and Cho metabolite values and Cho/NAA ratio over each brain lobar region for the control and the mTBI subject groups and each of the reconstruction methods are shown in Figure 7 for both WM and GM tissues. For simplicity, brain regions from only the left hemisphere are shown; right hemisphere regions showed similar trend. Relative to the controls, general findings by all three reconstruction methods indicate that in the WM: i) NAA was consistently lower in all lobar regions of the mTBI groups, and significant differences were found in all the lobes of the mTBI group except the temporal and occipital lobes detected by all three reconstruction methods; ii) similarly, Cho was consistently higher in all the lobar regions; iii) there was no clearly observable trend for Cre (data not shown, also see Table 1), and although increases were found in the right and left temporal and parietal lobes, the *p*-values were in the conservatively significant range of 0.015 to 0.067; and finally iv) Cho/NAA showed the most consistent and significant increases in all brain regions. A summary of findings for the GM measures, relative to the controls, include the following: i) NAA was slightly decreased in all but the left temporal lobe, reaching significance in the bilateral frontal and right occipital lobes for the full k-space data, and showed significant increase in the left temporal lobe by the GRAPPA and central k-space data that was considered a false positive for these methods; ii) Cho was consistently higher in all the lobar regions, except it was lower in the left occipital lobe for full and central k-space data and unchanged for GRAPAA; and finally iii) Cho/NAA followed the same trend

as the Cho, except in the left temporal region, was significantly increased in bilateral frontal and parietal lobes, with no significant differences found between the methods.

The results of GRAPPA and central k-space acquisitions demonstrate good agreement with those of fully sampled data in detecting differences in the mTBI group relative to the normal subjects. Assuming each method as an independent detector for the mTBI pathology, out of 54 assessed metabolic and regional brain segments (2 tissue types (GM/WM) × 9 brain regions × 3 metabolites and ratio), GRAPPA, central, and full showed 16, 18, and 17 statistically significant altered metabolites, respectively.

The results of the two-way ANOVA comparing the three reconstruction methods and the group differences in the 54 segments indicated that: i) non-significant differences between the three methods were found in 23 segments; ii) significant differences between the control group and the mTBI group were found in 16 segments; iii) only 5 significant interactions, in the left parietal GM NAA and Cho, right parietal GM NAA, and left occipital GM Cho/NAA and Cho were found between the type of method used and the specific group under investigation. Compared to the gold standard findings of the fully sampled data, the true positive and the true negative for GRAPPA were 15 and 35 and for central k-space were 15 and 34, respectively. This translates to a sensitivity of 88.23% and 88.23%, specificity of 95% and 91.9%, and accuracy of 92.6% and 90.7% for the GRAPPA and the central k-space reconstruction, respectively.

DISCUSSION AND CONCLUSIONS

Despite the use of echo-planar methods to increase sampling efficiency the data acquisition times for volumetric MRSI studies can become a limiting factor in the implementation of these methods for clinical studies. For this reason reduced k-space methods have been implemented to further reduce acquisition times; however, these methods also involve some decrease in SNR (6, 7) or increased artifacts relative to full k-space sampling, which may in turn affect the ability to obtain a clinical diagnosis. In this study, a reduced k-space acquisition was combined with an EPSI acquisition and reconstruction performed using a modified GRAPPA with phase correction algorithm. It was shown that proper implementation of parallel imaging of the 3D EPSI sequences can yield similar image quality and metabolite concentrations compared to results from the full k-space data leading to equivalent diagnostic decisions. Results confirm the decrease in SNR and as a consequence, the increased CRLB values for the reduced k-space measurements for the same voxel volume; however, with minimal impact on a between-group comparison based on regional mean metabolite value measurements. In some cases the acquired GRAPPA data showed superior results than the fully sampled k-space data (see Figure 3 and Table 1), which could arguably be due to the shorter scan times (16.4 min versus 26 min) of GRAPPA acquisition that makes it less susceptible to subject motion and other unwanted fluctuations; for example, a reduction in B0 drift from 7.5 Hz to 4.3 Hz was observed. In contrast, MRSI data reconstructed with central k-space EPSI had poorer spectral quality with noticeable residual signals and more variability, a finding that supports the use of higher-spatial encoding sizes. The number of voxels for which the fit process failed due to deterioration of spectral quality significantly increased, although the mean lobar metabolite concentrations of NAA, Cre, and Cho were not statistically different from the gold standard.

A number of time-saving PI-based MRSI methods have been already proposed and several basic spectral characteristics evaluated; however, the use of these techniques for clinical applications requires more evaluation and validation in terms of SNR, spectral variability and artifacts, and the impact of these characteristics on the metabolite levels, disease extent definition, and diagnostic accuracy. Ozturk-Isik *et al.* (10) showed the effectiveness of

SENSE parallel imaging combined with a spatially-limited MRSI in patients with high-grade glioma tumors. This pathology, however, poses modest diagnostic challenges for MRSI because of their distinct abnormality appearance on conventional MRI and significant alterations of the brain metabolites. In addition, the increased lipid contamination into the PRESS-selected volume, owing to the relatively small fields of view and matrix sizes associated with their SENSE MRSI method is also a concern. Other rapid volumetric MRSI approaches based on spiral acquisitions with (14) and without (28–30) the use of PI techniques have been introduced. However, through their radio frequency excitation pulses such acquisitions usually suffer from low SNR and artifacts, such as chemical-shift displacement error, nonuniform excitation, and lipid contamination. Optimized adiabatic pulses have been recently proposed that minimized these artifacts though clinical diagnostic feasibility was also demonstrated in patients with brain tumor (30).

This work has ascertained the roll of the GRAPPA parallel imaging technique applied to high resolution spectroscopic imaging intended for whole-brain volumetric analysis. The strong agreement between the spectral and spatial results of the acquired and the simulated GRAPPA acquisitions supports the use of reduced k-space EPSI data for clinical studies. It is known that the noise in data acquired with parallel imaging is not uniformly distributed; thus, the ability to quantify metabolites throughout the brain, including the cerebral cortex, and in neurological disorders that can have relatively subtle metabolic alterations, poses a challenge (20, 21, 31). However, little difference was found between the quantitative metabolites values and spectral line-width acquired with and without GRAPPA, despite the reduced SNR inherent to parallel imaging (6, 7). The high linear correlation and the proximity to the line of identity (slope = 1.0 and intercept = 0.0) between the GRAPPA results for the individual metabolites and the gold standard confirms the high reliability, unbiased, and robustness of the GRAPPA-EPSI approach implemented in this study. As a result, high specificity and sensitivity were obtained relative to the fully sampled MRSI data of alerted metabolites in group of mTBI patients; and in good agreement with previous findings (21). In contrast, the central k-space method was less specific in detecting the altered metabolites. This likely resulted from the deterioration of spectral line shapes and larger voxels, which makes the acquisition more susceptible to the magnetic field inhomogeneity and lipid contamination (32) but maintains SNR (Figures 3–4 and Table 1).

The ratio of Cho/NAA, or NAA/Cho, is commonly used to increase the sensitivity for detecting changes seen after brain injury, as NAA and Cho often vary in opposite directions, and this is also clearly detected by all reconstruction methods used in this study (reaching a 100% agreement), in which significant increases were found in both GM and WM. While Cre was found to be increased in temporal and parietal WM and two GM regions, these differences were small, which is consistent with our previous findings. As such, the analysis of the Cre metabolite was not carried forward for the comparisons between the control and the mTBI groups, although voxel-based and lobar-based between-method linear regression analyses were performed for each group separately which concluded nearly identical Cre values.

One limitation of this study is the assumption of the fully sampled data as the reference gold standard against which our reduced k-space metabolites concentrations and statistical outcomes were compared. In practice, this assumption is not necessarily true because the GRAPPA acquisition can be less prone to temporal instabilities, therefore potentially improving the data quality. Hence, the method could be relatively more robust, *i.e.*, with less numbers of failed exams compared to the lengthier full EPSI scans. Therefore, one possible reason for the observation of a greater number of fitted voxels in the reduced k-space data compared to the fully sampled data in mTBI subjects (Table 1) could be due to removal of motion-corrupted samples in the simulations. An additional limitation is that paired

comparisons between the mTBI and normal subject groups were only performed for the same 3D EPSI reconstruction method. Since only a small interaction was found between the group and the method used (5 out 54, ~ 9%, with conservatively significant *p*-values between 0.015 and 0.042), we believe this is sufficient.

Given the diffuse metabolites alterations in mild brain injuries (20, 21), this study has additionally shown that the PI-enabled MRSI methodology with voxel-based analysis of individual subject whole-brain metabolite data and comparison with normative metabolite data (22) can potentially provide quantitative information comparable to the fully sampled MRSI data used in the diagnosis and evaluation of neurological disorders. The ability to distinguish between these study groups is also dependent on instrumental factors, for which we note that the sensitivity obtained by the use of 3-Tesla and an 8-channel receiver coil was sufficient to make up for the reduction in SNR for the GRAPPA acquisitions (7). Additional improvements can potentially be obtained by using a receive coil with a higher number of elements and/or MRSI acquisitions with shorter echo times (13, 33) that would enable the 3D EPSI GRAPPA acquisition to be further accelerated.

In conclusion, this study has demonstrated that the GRAPPA parallel imaging method implemented for a volumetric EPSI acquisition of whole-brain, high-resolution metabolite maps, has been shown to result in reduced SNR although with comparable findings for discrimination of mild TBI relative to the fully sampled MRSI acquisition.

Acknowledgments

Grant Support: National Institutes of Health (grants R01NS055107 and R01EB000822)

REFERENCES

1. Kurhanewicz J, Vigneron DB, Nelson SJ. Three-dimensional magnetic resonance spectroscopic imaging of brain and prostate cancer. Neoplasia. 2000; 2(1–2):166–189. [PubMed: 10933075]
2. Tedeschi, Bertolino A, Righini A, Campbell G, Raman R, Duyn JH, Moore C, Alger JR, Di Chiro G. Brain regional distribution pattern of metabolite signal intensities in young adults by proton magnetic resonance spectroscopic imaging. Neurology. 1995; 45(7):1384–1391. [PubMed: 7617201]
3. Bertolino A, Callicott JH, Nawroz S, Mattay VS, Duyn JH, Tedeschi G, Frank JA, Weinberger DR. Reproducibility of proton magnetic resonance spectroscopic imaging in patients with schizophrenia. Neuropsychopharmacology. 1998; 18:1–9. [PubMed: 9408913]
4. Posse S, DeCarli C, Le Bihan D. Three-dimensional echo-planar MR spectroscopic imaging at short echo times in the human brain. Radiology. 1994; 192:733–738. [PubMed: 8058941]
5. Sodickson DK, Manning WJ. Simultaneous acquisition of spatial harmonics (SMASH): fast imaging with radiofrequency coil arrays. Magn Reson Med. 1997; 38(4):591–603. [PubMed: 9324327]
6. Pruessmann KP, Weiger M, Scheidegger MB, Boesiger P. SENSE: sensitivity encoding for fast MRI. Magn Reson Med. 1999; 42(5):952–962. [PubMed: 10542355]
7. Griswold MA, Jakob PM, Heidemann RM, Nittka M, Jellus V, Wang J, Kiefer B, Haase A. Generalized autocalibrating partially parallel acquisitions (GRAPPA). Magn Reson Med. 2002; 47(6):1202–1210. [PubMed: 12111967]
8. Dydak U, Weiger M, Pruessmann KP, Meier D, Boesiger P. Sensitivity-encoded spectroscopic imaging. Magn Reson Med. 2001; 46(4):713–722. [PubMed: 11590648]
9. Dydak U, Pruessmann KP, Weiger M, Tsao J, Meier D, Boesiger P. Parallel spectroscopic imaging with spin-echo trains. Magn Reson Med. 2003; 50(1):196–200. [PubMed: 12815695]
10. Ozturk-Isik E, Chen AP, Crane JC, Bian W, Xu D, Han ET, Chang SM, Vigneron DB, Nelson SJ. 3D sensitivity encoded ellipsoidal MR spectroscopic imaging of gliomas at 3T. Magn Reson Imaging. 2009; 27(9):1249–1257. [PubMed: 19766422]

11. Lin FH, Tsai SY, Otazo R, Caprihan A, Wald LL, Belliveau JW, Posse S. Sensitivity-encoded (SENSE) proton echo-planar spectroscopic imaging (PEPSI) in the human brain. Magn Reson Med. 2007; 57(2):249–257. [PubMed: 17260356]
12. Zhu X, Ebel A, Ji JX, Schuff N. Spectral phase-corrected GRAPPA reconstruction of three-dimensional echo-planar spectroscopic imaging (3D-EPSI). Magn Reson Med. 2007; 57(5):815–820. [PubMed: 17457872]
13. Tsai SY, Otazo R, Posse S, Lin YR, Chung HW, Wald LL, Wiggins GC, Lin FH. Accelerated proton echo planar spectroscopic imaging (PEPSI) using GRAPPA with a 32-channel phased-array coil. Magn Reson Med. 2008; 59(5):989–998. [PubMed: 18429025]
14. Gu M, Liu C, Spielman DM. Parallel spectroscopic imaging reconstruction with arbitrary trajectories using k-space sparse matrices. Magn Reson Med. 2009; 61(2):267–272. [PubMed: 19165883]
15. Mayer D, Kim DH, Spielman DM, Bammer R. Fast parallel spiral chemical shift imaging at 3T using iterative SENSE reconstruction. Magn Reson Med. 2008; 59(4):891–897. [PubMed: 18383298]
16. Posse S, Otazo R, Tsai SY, Yoshimoto AE, Lin FH. Single-shot magnetic resonance spectroscopic imaging with partial parallel imaging. Magn Reson Med. 2009; 61(3):541–547. [PubMed: 19097245]
17. Blaimer M, Breuer FA, Mueller M, Seiberlich N, Ebel D, Heidemann RM, Griswold MA, Jakob PM. 2D-GRAPPA-operator for faster 3D parallel MRI. Magn Reson Med. 2006; 56(6):1359–1364. [PubMed: 17058204]
18. Rueckert, M.; Otazo, R.; Posse, S. ISMRM: 2006. 2006. GRAPPA Reconstruction of Sensitivity Encoded 2D and 3D Proton Echo Planar Spectroscopic Imaging (PEPSI) with SNR Adaptive Recalibrating; p. 296
19. Zierhut ML, Ozturk-Isik E, Chen AP, Park I, Vigneron DB, Nelson SJ. (1)H spectroscopic imaging of human brain at 3 Tesla: comparison of fast three-dimensional magnetic resonance spectroscopic imaging techniques. J Magn Reson Imaging. 2009; 30(3):473–480. [PubMed: 19711396]
20. Signoretti S, Di Pietro V, Vagnozzi R, Lazzarino G, Amorini AM, Belli A, D'Urso S, Tavazzi B. Transient alterations of creatine, creatine phosphate, N-acetylaspartate and high-energy phosphates after mild traumatic brain injury in the rat. Mol Cell Biochem. 2009
21. Govind V, Gold S, Kaliannan K, Saigal G, Falcone S, Arheart KL, Harris L, Jagid J, Maudsley AA. Whole-brain proton MR spectroscopic imaging of mild-to-moderate traumatic brain injury and correlation with neuropsychological deficits. Journal of Neurotrauma. 2010; 27(3):483–496. [PubMed: 20201668]
22. Maudsley AA, Domenig C, Govind V, Darkazanli A, Studholme C, Arheart K, Bloomer C. Mapping of brain metabolite distributions by volumetric proton MR spectroscopic imaging (MRSI). Magnetic Resonance in Medicine. 2009; 61(3):548–559. [PubMed: 19111009]
23. Maudsley AA, Darkazanli A, Alger JR, Hall LO, Schuff N, Studholme C, Yu Y, Ebel A, Frew A, Goldgof D, et al. Comprehensive processing, display and analysis for in vivo MR spectroscopic imaging. NMR in Biomedicine. 2006; 19(4):492–503. [PubMed: 16763967]
24. Sodickson DK. Tailored SMASH image reconstructions for robust in vivo parallel MR imaging. Magn Reson Med. 2000; 44(2):243–251. [PubMed: 10918323]
25. Brown MA. Time-domain combination of MR spectroscopy data acquired using phased-array coils. Magn Reson Med. 2004; 52(5):1207–1213. [PubMed: 15508170]
26. Collins DL, Zijdenbos AP, Kollokian V, Sled JG, Kabani NJ, Holmes CJ, Evans AC. Design and construction of a realistic digital brain phantom. IEEE Transactions on Medical Imaging. 1998; 17:463–468. [PubMed: 9735909]
27. Provencher SW. Estimation of metabolite concentrations from localized in vivo proton NMR spectra. Magnetic Resonance in Medicine. 1993; 30(6):672–679. [PubMed: 8139448]
28. Adalsteinsson E, Irarrazabal P, Spielman DM, Macovski A. Three-dimensional spectroscopic imaging with time-varying gradients. Magnetic Resonance in Medicine. 1995; 33:461–466. [PubMed: 7776875]

29. Adalsteinsson E, Irarrazabal P, Topp S, Meyer C, Macovski A, Spielman DM. Volumetric spectroscopic imaging with spiral-based k-space trajectories. Magnetic Resonance in Medicine. 1998; 39:889–898. [PubMed: 9621912]

30. Andronesi OC, Gagoski BA, Sorensen AG. Neurologic 3D MR spectroscopic imaging with low-power adiabatic pulses and fast spiral acquisition. Radiology. 2012; 262(2):647–661. [PubMed: 22187628]

31. Signoretti S, Marmarou A, Fatouros P, Hoyle R, Beaumont A, Sawauchi S, Bullock R, Young H. Application of chemical shift imaging for measurement of NAA in head injured patients. Acta Neurochir Suppl. 2002; 81:373–375. [PubMed: 12168350]

32. Ebel A, Maudsley AA. Improved spectral quality for 3D MR spectroscopic imaging using a high spatial resolution acquisition strategy. Magn Reson Imaging. 2003; 21(2):113–120. [PubMed: 12670597]

33. Otazo R, Tsai SY, Lin FH, Posse S. Accelerated short-TE 3D proton echo-planar spectroscopic imaging using 2D-SENSE with a 32-channel array coil. Magn Reson Med. 2007; 58(6):1107–1116. [PubMed: 17968995]

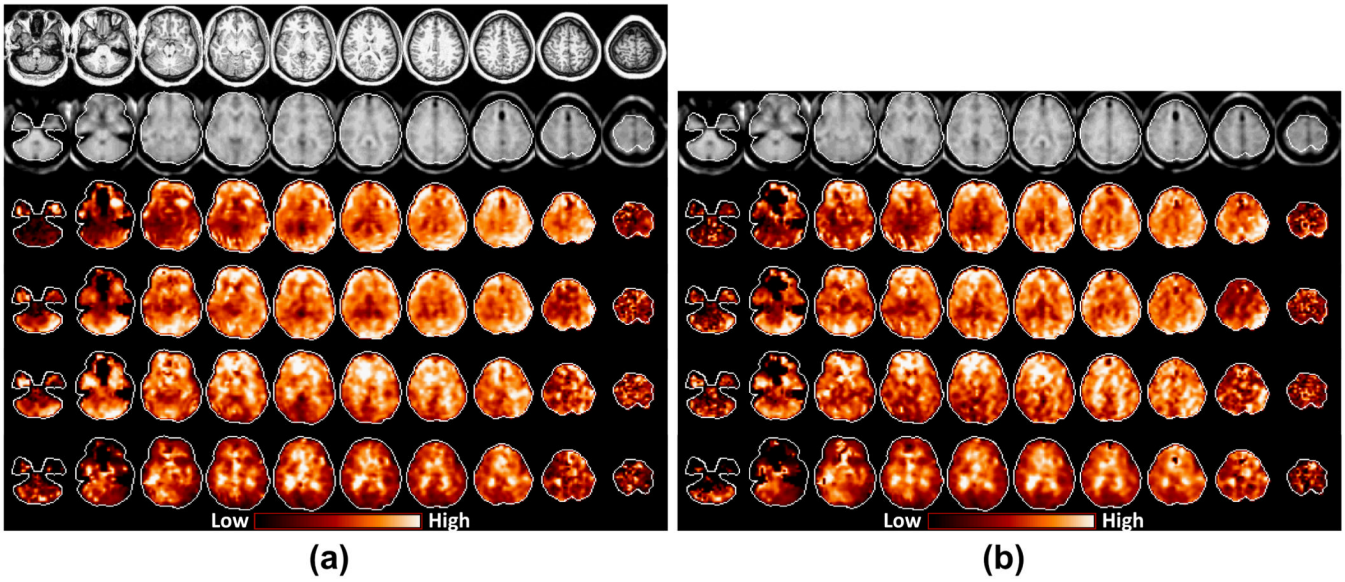

Figure 1.

Structural and metabolite images obtained from a healthy normal subject (Group 1) using (a) the fully sampled EPSI and (b) the GRAPPA-EPSI sequences. Images in from top to bottom rows are: axial T1-weighted MRI (corresponding to 5-mm slice thickness and matched to SI slice location), SI-resolution interleaved water reference, NAA, Cre, Cho, and Cho/NAA, respectively (NAA: N-acetyl aspartate; Cre: creatine; Cho: choline).

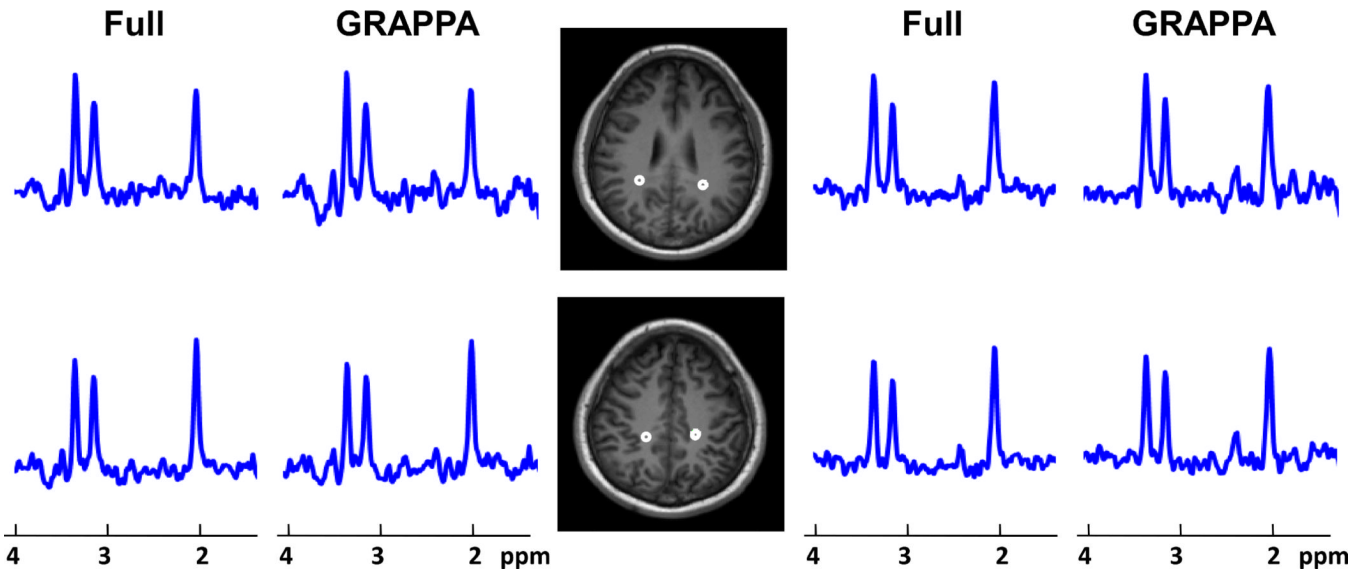

Figure 2.

Comparison between representative spectra from the GRAPPA and the fully sampled MRSI obtained from a 22-year-old male subject with mild traumatic brain injury. Spectra were obtained from the regions indicated on the MRIs and are shown at a fixed vertical scale. Compare to an aged-matched control subject (see Figure 3), both GRAPPA and fully sampled data indicate Cho increase in both slices and NAA reduction in the inferior slice.

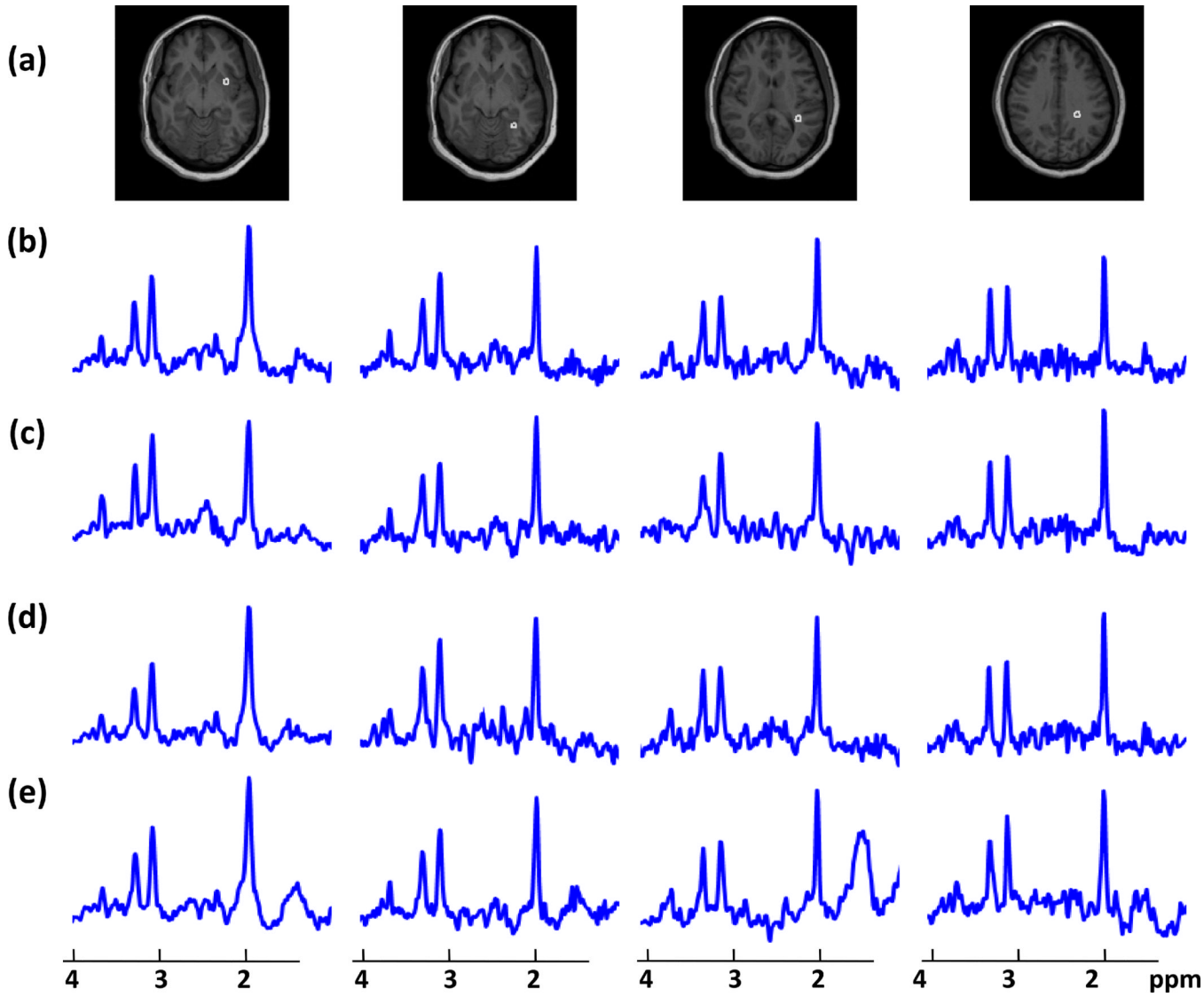

Figure 3.
T1-weighted MRI (a) showing voxel locations for MR spectra of a 25-year-old normal subject at four different SI slices reconstructed using (b) full k-space, (c) acquired GRAPPA (d) simulated GRAPPA, with an acceleration factor of 1.5, and (e) central k-space data.

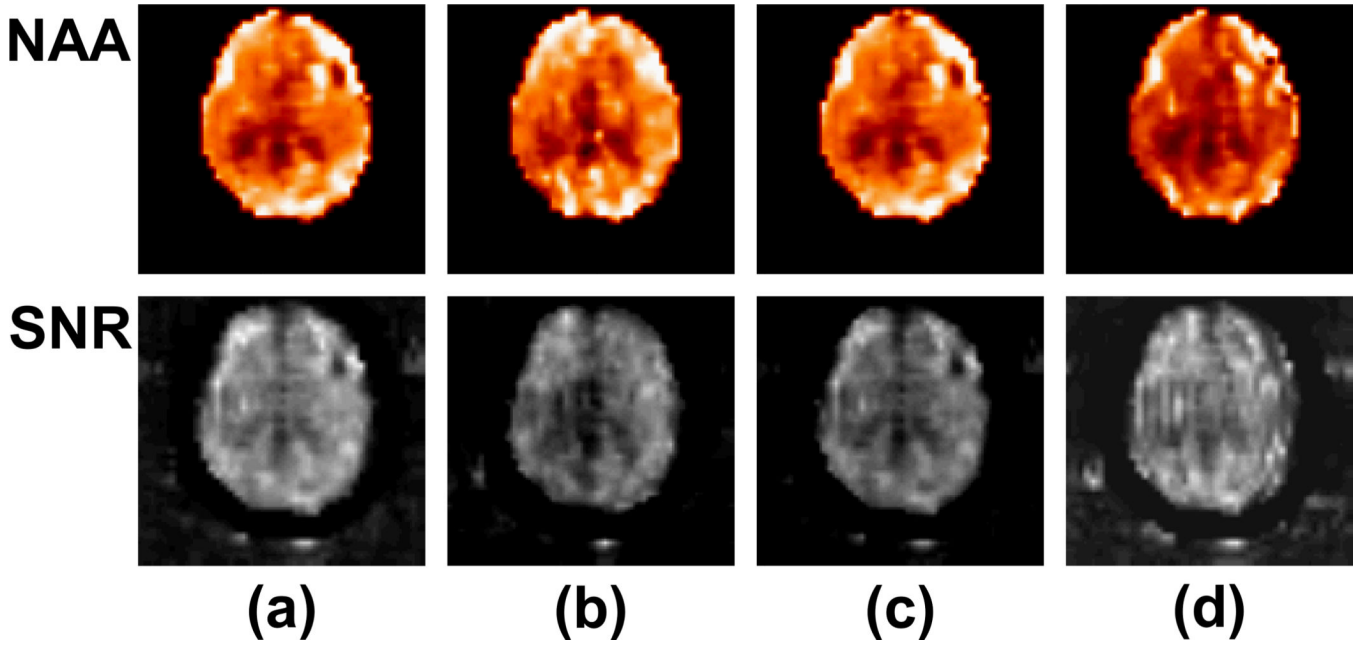

Figure 4.
Representative maps of NAA metabolite and the SNR for NAA for the four different reconstruction methods: (a) fully sampled data, (b) acquired GRAPPA, (c) simulated GRAPPA, and (d) central k-space displayed at the same level of brightness and contrast.

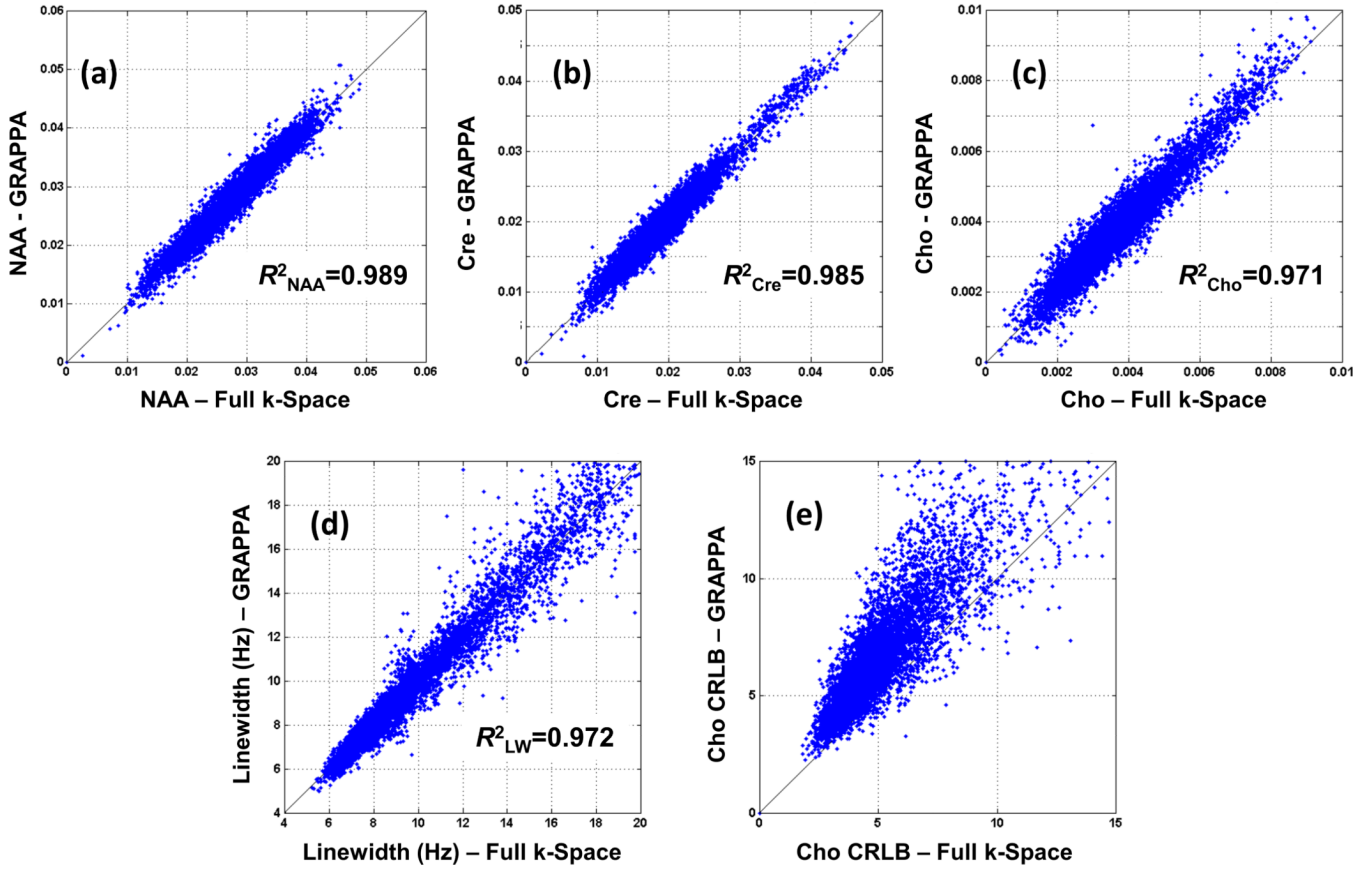

Figure 5.

Voxel metabolites concentrations from the whole-brain of a normal subject (Group 1) from GRAPPA-EPSI plotted against those obtained with full k-space EPSI for (a) NAA, (b) Cre, and (c) Cho. NAA spectral line-width comparison is also shown in (d) and the CRLB values for Cho is shown in (e).

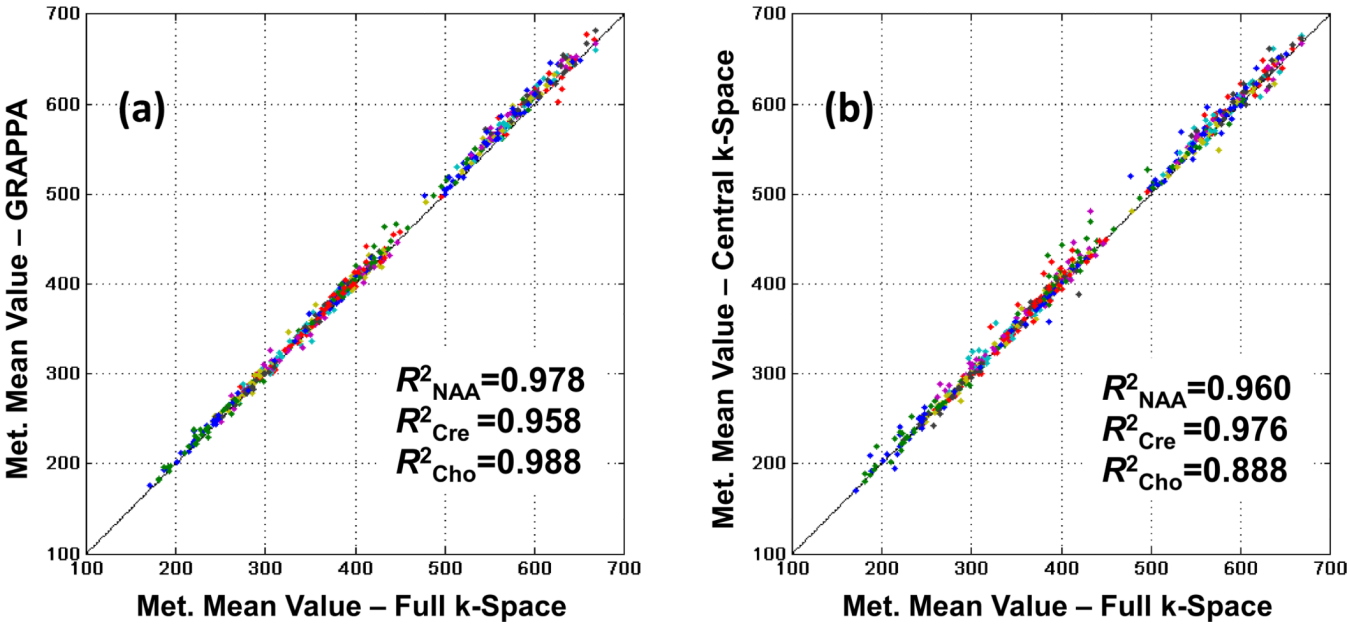

Figure 6.

Mean metabolites concentrations in institutional unit from the nine atlas-registered brain lobes (left and right frontal, temporal, parietal and occipital, and cerebellum) of the mTBI subjects group from (a) GRAPPA-EPSI and (b) central k-space plotted against those obtained with fully sampled k-space EPSI.

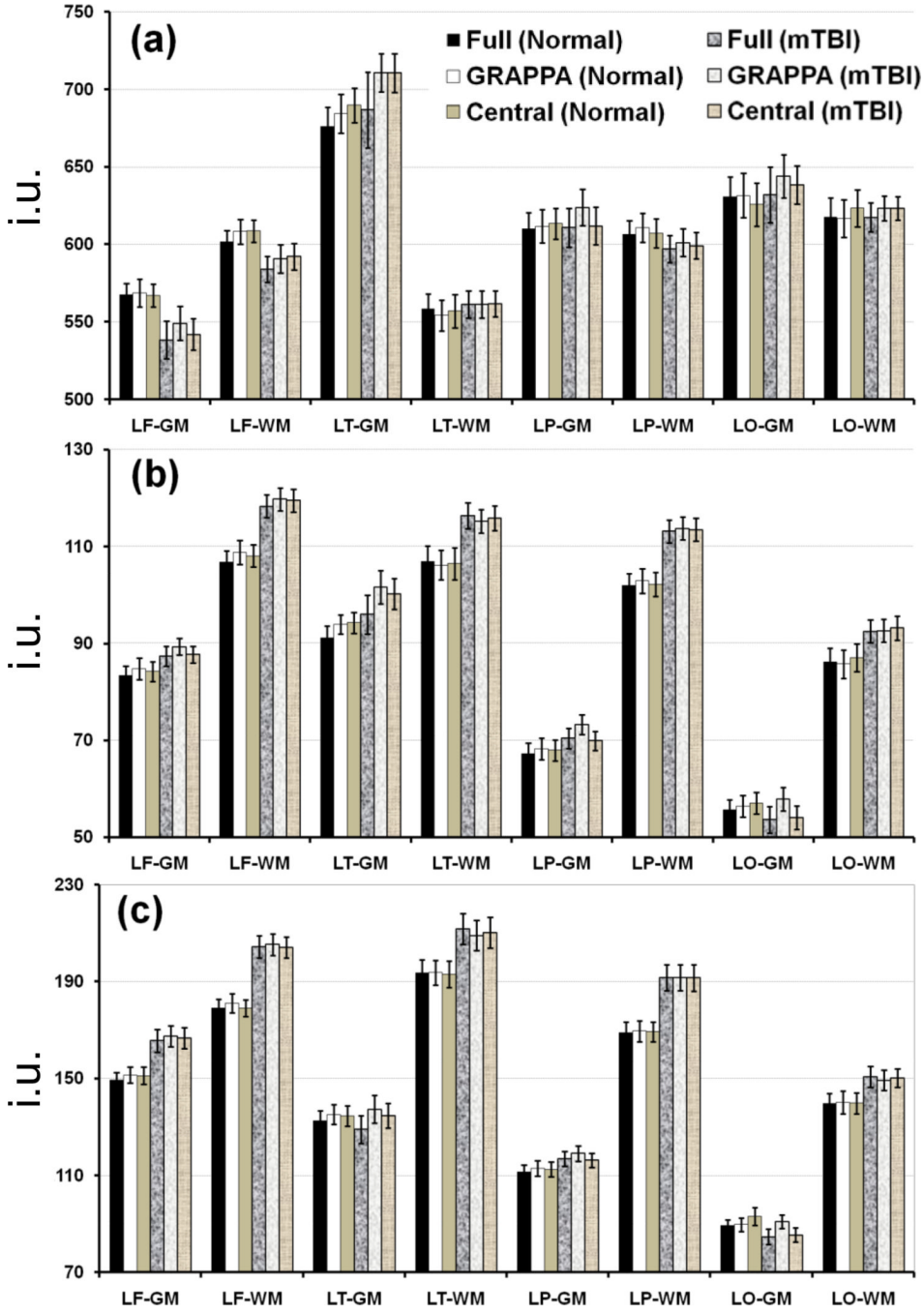

Figure 7.

Mean values of the NAA and Cho metabolites and Cho/NAA ratio in the gray and white matters (GM/WM) of control and mTBI groups, by brain region, with error bars for 1.0 standard error. For simplicity, brain regions from only the left hemisphere are shown. Data are reconstructed by fully sampled k-space (dark bars), GRAPPA (white bars), and central k-space (light bars) and shown for control (solid bars) and mTBI (hashed/textured bars) groups. The y-axis scale for the metabolite values is in institutional unit (i.u.). Abbreviations used for the hemispheric lobar regions are: the first letter L indicates the left side of the brain, and the second letter F/T/P/O indicates frontal/temporal/parietal/occipital lobes, respectively.

Table 1

Spectral quality in terms of fitted volume percentage, mean metabolite concentrations averaged over all voxels of white matter brain tissue in parietal lobe, and signal-to-noise ratio (SNR) for 3D EPSI reconstructed using full k-space, GRAPPA, and central k-space data.

Data	Acquisition	Fitted Volume (%)	NAA	Cre	Cho	SNR
Normal	*Full k-space*	72.5+3.15	591±36.6	348±22.9	99±8.1	22.5±2.82
(Group1)	*Acq-GRAPPA*	71.5+2.89	595±37.9	346±23.9	100±9.7	16.7±2.78
	Sim-GRAPPA	72.0+2.97	592±38.2	341±25.4	97±9.1	17.0±2.14
	Central k-space	65.7+2.66	588±39.0	347±26.0	98±9.9	21.5±3.11
Normal	*Full k-space*	71.7+2.35	585±35.6	338±23.9	97±9.6	20.0±2.39
(Group2)	*Sim-GRAPPA*	69.1+2.44	591±35.2	343±23.6	99±9.0	14.7±2.08
	Central k-space	68.6+2.46	589±37.1	342±24.2	98±9.6	19.0±2.74
mTBI	*Full k-space*	64.3+3.35	577±42.5	357±26.4	110±11.1	18.7±1.48
	Sim-GRAPPA	65.5+2.63	585±39.4	360±28.1	111±11.7	15.1±1.39
	Central k-space	65.6+2.36	584±39.6	359±25.7	110±11.0	18.5±1.71